Polymer Chemistry

PAPER

View Article Online
View Journal | View Issue

Cite this: *Polym. Chem.*, 2015, **6**, 973

Solution processible hyperbranched inverse-vulcanized polymers as new cathode materials in Li–S batteries†

Yangyang Wei,[a] Xiang Li,[b] Zhen Xu,[a] Haiyan Sun,[a] Yaochen Zheng,[a,c] Li Peng,[a] Zheng Liu,[a] Chao Gao*[a] and Mingxia Gao*[b]

Received 24th September 2014,
Accepted 14th October 2014

DOI: 10.1039/c4py01055h

www.rsc.org/polymers

Soluble inverse-vulcanized hyperbranched polymers (SIVHPs) were synthesized *via* thiol–ene addition of polymeric sulfur (S_8) radicals to 1,3-diisopropenylbenzene (DIB). Benefiting from their branched molecular architecture, SIVHPs presented excellent solubility in polar organic solvents with an ultrahigh concentration of 400 mg mL^{-1}. After end-capping by sequential click chemistry of thiol–ene and Menschutkin quaternization reactions, we obtained water soluble SIVHPs for the first time. The sulfur-rich SIVHPs were employed as solution processible cathode-active materials for Li–S batteries, by facile fluid infiltration into conductive frameworks of graphene-based ultralight aerogels (GUAs). The SIVHPs-based cells showed high initial specific capacities of 1247.6 mA h g^{-1} with 400 charge–discharge cycles. The cells also demonstrated an excellent rate capability and a considerable depression of shuttle effect with stable coulombic efficiency of around 100%. The electrochemical performance of SIVHP in Li–S batteries overwhelmed the case of neat sulfur, due to the chemical fixation of sulfur. The combination of high solubility, structure flexibility, and superior electrochemical performance opens a door for the promising application of SIVHPs.

Introduction

Hyperbranched polymers (HPs) have attracted wide attention due to their distinctive chemical and physical properties, which are derived from their unique three-dimensional dendritic molecular architecture with high content of functional groups, low viscosity and high solubility.[1] HPs have been applied in some fields including coatings, processing additives and electrolytes in lithium ion batteries.[2] However, HPs have never been used as electrode materials, probably due to the difficulty in the design of the desired molecular structures.

On the other hand, the Li–S battery is emerging as a new kind of lithium ion battery. Organosulfur compounds and sulfurized carbons are being explored to be used as cathode materials in lithium ion batteries, aimed at exceeding the performance of marketable products like $LiCoO_2$ and $LiMnO_2$.[3] However, the energy density of Li–S batteries of this kind was hard to improve since it was fairly difficult to obtain organosulfur compounds and sulfurized carbons with sulfur content over 50 wt%.[4] Additionally, sulfurized carbons usually need tedious thermal treatments above 250 °C, due to their poor solubility.[5] Recently, Pyun and co-workers addressed such a challenge *via* bulk inverse vulcanization, which was the copolymerization of a large percentage of sulfur (50–99 wt%) and a modest amount of DIB (1–50 wt%). It exhibited high specific capacity and stability when using these copolymers as cathode-active materials in Li–S batteries.[6] However, partial solubility led to hard processability below the thermal decomposition temperature of these polymers. Therefore, polymers with high sulfur content and high solubility are eagerly expected.

Herein, we synthesized a kind of SIVHPs *via* thiol–ene addition of S_8 radicals to DIB in solution. These SIVHPs possess relatively high molecular weights and excellent solubility in organic solvents (up to 400 mg mL^{-1}). When modified *via* sequential thiol–ene and Menschutkin click reactions,

[a]*MOE Key Laboratory of Macromolecular Synthesis and Functionalization, Department of Polymer Science and Engineering, Zhejiang University, 38 Zheda Road, Hangzhou, P. R. China. E-mail: chaogao@zju.edu.cn*
[b]*State Key Laboratory of Silicon Materials, Key Laboratory of Advanced Materials and Applications for Batteries of Zhejiang Province & Department of Materials Science and Engineering, Zhejiang University, Hangzhou 310027, PR China. E-mail: gaomx@zju.edu.cn; Tel: +86-571-87952615*
[c]*College of Chemistry and Chemical Engineering, Yantai University, 30 Qingquan Road, Yantai 264005, P. R. China*

†Electronic supplementary information (ESI) available: Data of molar masses before and after modification of SIVHPs, solubility of SIVHPs in electrolyte, GPC curves of SIVHPs, differential scanning calorimetry for preparation of SIVHPs, FTIR spectra, TGA curves and EIS spectra for SIVHPs. See DOI: 10.1039/c4py01055h

SIVHPs were endowed with water solubility for the first time. The solution of SIVHPs in $CHCl_3$ was absorbed into GUAs[7] and used as a cathode-active material in Li–S batteries. The Li–S batteries showed high coulombic efficiency (~100%), superior cycling performance and good rate capability.

Experimental

Materials

DIB and 2,2-dimethoxy-2-phenyl-acetophenone (DMPA) were purchased from TCI Shanghai. 3-(Dimethylamino)-1-propanethiol was acquired from Atomax Chem Co. Ltd Sublimed sulfur, chloroform ($CHCl_3$), dimethylformamide (DMF), tetrahydrofuran (THF), toluene, 1,4-dioxane, anisole, *N*-methyl-2-pyrrolidone (NMP) and other organic solvents were purchased from Sinopharm Chemical Reagent Co. Ltd DIB was passed through a column of basic alumina before using and all the other materials were used as received.

Instrumentation

Gel permeation chromatography (GPC) was recorded on a PerkinElmer HP 1100, using THF as the eluent at a flow rate of 1 mL min^{-1}, RI-WAT 150 CVt+ as the detector and linear polystyrene for calibration at 40 °C for characterization of apparent molecular weights. ^{1}H NMR (400 MHz) spectroscopy measurements were carried out on a Varian Mercury Plus 400 NMR spectrometer. ^{13}C NMR (500 MHz) measurements were carried out on an Avance III 500 NMR spectrometer. Fourier transform infrared (FTIR) spectra were recorded on a PE Paragon 1000 spectrometer (film or KBr disk). UV-visible spectra were obtained using a Varian Cary 300 Bio UV-visible spectrophotometer. Thermogravimetric analysis (TGA) was carried out on a PerkinElmer Pyris 6 TGA instrument under nitrogen with a heating rate of 10 °C min^{-1}. SEM images were obtained by a Hitachi S4800 field-emission SEM system. The cells were discharged and charged on a LAND electrochemical station (Wuhan) from 1.0 to 3.0 V at a current density of 100 mA g^{-1} sulfur to test the cycle life. Cyclic voltammograms (CV) were recorded on a CHI604c electrochemical workstation (Shanghai Chenhua) between 1.0 and 3.0 V to characterize the redox behavior and the kinetic reversibility of the cell. Electrochemical impedance spectrum (EIS) measurements were performed using a frequency response analyzer (Solartron 1255B, Solartron) equipped with an electrochemical interface (1287, Solartron) in a frequency range of 100 kHz to 0.01 Hz and a potentiostatic signal amplitude of 5 mV. Prior to the EIS measurement, the cell was activated by three cycles at 0.1 C between 1.5–3.0 V *vs.* Li^+/Li. All of the electrochemical tests were performed at 25 ± 1 °C. The dissolution behavior of the SIVHPs in electrolyte was determined after soaking SIVHPs for 48 h. After soaking, the insoluble part of the SIVHPs was dried at 50 °C in a vacuum oven. The weight percentage of the soluble part was calculated using the following equation:

$$W = \frac{m_0 - m_1}{m_0} \times 100\%$$

where W is the solubility of SIVHPs, m_0 is the mass of SIVHPs (g) and m_1 is the mass of the insoluble part of SIVHPs (g).[8]

Synthesis of soluble inverse-vulcanized hyperbranched polymers *via* thiol–ene addition of S_8 radicals to DIB in solution

S_8 and DIB were mixed in $CHCl_3$ (or toluene, *etc.*) with feed molar ratios of S_8 to DIB from 2 to 8 (8, 4, 8/3, 2 and 8/5). The volume of solvent was calculated to get a mass fraction of reactants of 35%. The reaction took place in an autoclave under N_2 atmosphere followed by heating to 150 °C–180 °C (150, 160, 170, 180, 190 and 200 °C) for 0.5–7 hours (0.25, 0.5, 0.75, 1, 2, 3, 5, 7 hours). After cooling down to room temperature, the solution was precipitated with *n*-hexane. After being dried at 80 °C, the orange-red product was achieved (yield: 35%–80%). ^{1}H NMR (400 MHz, $CDCl_3$), δ (ppm): 7.32 (C_6H_4), 5.63–4.94 (C=CH_2), 4.26–2.48 (S_n–CH_2–C), 2.37–0.44 (C–CH_3). ^{13}C NMR (500 MHz, $CDCl_3$), δ (ppm): 146.5–137.1, 129.9–120.5, 117.6, 112.8, 59.4–41.5, 33.7–11.6. FTIR: 2967.24 (C–H), 1598.24 (C=C), 1537.32–1340.99 (C–H), 1213.91 (C–C), 855.08–650.48 (C–H), 486.50 (C–S) cm^{-1}.

Synthesis of quaternary ammonium SIVHPs

SIVHPs (0.04 g, 1 mmol), 3-(dimethylamino)-1-propanethiol (DPT) (0.60 g, 5 mmol) and DMPA (21 mg, 0.08 mmol) were added into dried toluene (2 mL) in a 25 mL round-bottom flask. After being sealed, the mixture was bubbled with N_2 for 15 min to eliminate oxygen. Then, the reaction was triggered by UV-irradiation at 365 nm for 4 hours under stirring at room temperature. The solution was subsequently diluted with 8 mL of dried DMF and cooled down to 0 °C. Another DMF (3 mL) solution of 3-bromo-1-propyne (14 mg, 1.2 mmol) was added into the DMF solution above dropwise under vigorous stirring. The mixture was further stirred overnight and added into diethyl ether solution dropwise for precipitation at 0 °C to attain orange precipitates. After being dried in vacuum at room temperature, quaternary ammonium SIVHPs were achieved (yield: 50%–80%). ^{1}H NMR (400 MHz, DMSO), δ (ppm): 7.94–7.24 (C_6H_4), 4.00–3.73 (2H, CH_2–C≡CH), 3.60–3.39 (2H, C_6H_4–CH_2–CH_2–CH_2–N^+), 3.24–3.00 (7H, C≡CH, $N^+(CH_3)_2$), 3.00–2.92 (2H, C_6H_4–CH–CH_2–S), 2.85–2.73 (2H, S–CH_2–CH_2–CH_2–N^+), 2.25–1.96 (4H, C_6H_4–CH_2–CH_2–S, S–CH_2–CH_2–CH_2–N^+). ^{13}C NMR (500 MHz, DMSO), δ (ppm): 145.3–121.7, 82.8, 72.0, 61.7, 53.3, 49.8, 34.5, 33.7, 21.6–21.3.

Preparation of GUAs *via* the "sol-cryo" method

Graphene oxide was prepared by chemical exfoliation of graphite according to the previous protocol.[9] Typically, the aqueous graphene oxide and CNTs with the same concentration of 6.0 mg mL^{-1} were mixed and stirred with a magnetic bar for 1.5 h, and then poured into a mold followed by freeze-drying for 2 days. The as-prepared GO/CNTs foam has a known density of 6.0 mg mL^{-1}. After being chemically reduced by hydrazine vapor at 90 °C for 24 h and then vacuum-dried at 90 °C for 24 h, GUAs were achieved.[7]

Fabrication of Li–S batteries and electrochemical measurements

SIVHP (0.85 g) in 10 mL of $CHCl_3$ were added into GUAs (0.15 g) dropwise. The as-made materials were dried in a vacuum oven at 40 °C for 12 h to remove the solvent. The SIVHP-GUAs were mixed with poly(vinylidene fluoride) (PVDF 900), acetylene black (AB), and *N*-methyl-2-pyrrolidinone (NMP, anhydrous) to form a cathode slurry. The ratio of SIVHP-GUAs : AB : PVDF was 7.5 : 1 : 1.5 by weight. After mixing homogeneously overnight by magnetic stirring, the slurry was cast onto an aluminium current collector using a doctor blade. The control sulfur-GUAs cathode containing 60 wt% sulfur-GUAs, 20 wt% AB and 20 wt% PVDF binder was prepared in the same way. The control SIVHPs cathode containing 50 wt% SIVHPs, 35 wt% AB and 15 wt% PVDF binder was also prepared in the same way. The coated electrodes were dried in an oven at 60 °C for 24 h under ordinary pressure, and then in a vacuum oven at 60 °C for 24 h. Subsequently, the electrode was cut into disks with a diameter of 11 mm. Coin-type (CR2025) cells were assembled in an argon-filled glove box to avoid contamination by moisture and oxygen. The electrolyte used in this work was 1 mol L^{-1} LiTFSI in a solvent mixture of 1,3-dioxolane (DOL) and dimethoxymethane (DME) (1 : 1 v/v).

Results and discussion

Synthesis and characterization of SIVHPs *via* thiol–ene addition of S_8 radicals to DIB in solution

In the thiol–ene addition of S_8 radicals to DIB in solution to synthesize SIVHPs, S_8 and DIB were chosen as A_2 and B_4 monomers. The diradical moiety from thermal fracture of S_8 could react with the C=C bonds of DIB, as shown in Scheme 1.[10] S–S bonds were subjected to reversible rupture and formation during the reaction processes. Along with the increasing viscosity during polymerization, the movements of free radicals were obstructed, and the main trend of chain growth was gradually replaced by chain rupture.[11] We can infer that low viscosity together with relatively strong free radical activity afforded large molecular weights and a high degree of branching. This was the reason why polymerization in solution environment was preferred over bulk polymerization. Meanwhile, the branching molecular architecture should endow HPs with better solubility than copolymers by bulk polymerization.

After the polymerization, SIVHPs with relatively high molecular weight were obtained. Polymerization data were gained *via* GPC (Table 1), and feed molar ratio-, reaction time-, and temperature-dependent GPC curves are presented in Fig. S1,† showing the influence of reaction parameters. The polymerization in solution afforded the SIVHPs with the largest M_n of 5400 g $mol^{-1}$and M_w of 23 500 g mol^{-1} when the reaction parameters were set as 180 °C, 0.5 hour, and 4 as the feed molar ratio of S_8 to DIB. When the temperature and reaction time increased, molecular weight increased at the beginning and then decreased (Fig. S1a, 1b, 1d and 1e†), which is likely due to the rupture of S–S bonds. We also found that the polydispersity index (PDI) increased together with the molecular weight (Table 1), which indirectly proved the hyperbranched polymerization of SIVHPs.[12] Due to the advantages of solution polymerization mentioned above, SIVHPs with relatively high molecular weight and stable hyperbranched structure were obtained.

The structure of the resulting SIVHPs was characterized *via* ^1H NMR and ^{13}C NMR spectroscopy shown in Fig. 1a and 1b. In the ^1H NMR spectrum (Fig. 1a), the proton signal of the methylene group (labelled as "a") was observed at 2.48–4.26 ppm, which was influenced by the lengths of the linear polysulfane chains linked to the methylene group. It indicated that C–S bonds were successfully formed.[13] In the ^{13}C NMR spectrum (Fig. 1b), the methylene carbon signal (labelled as "a, c") which was located at 41.54–59.42 ppm implied the existence of C–S bonds. Notably, the signal split into two at around 44.25 ppm and 54.65 ppm, maybe due to the electron withdrawing effect of linear polysulfane with different lengths. FTIR spectra of monomer and SIVHP are also presented in Fig. S3,† in which the signal at 486.50 cm^{-1} belonged to C–S bonds.[14] In addition, UV-vis spectra of DIB and SIVHPs are shown in Fig. 2a for comparison. Compared with the pure DIB peak at 246 nm, the wider peak at 240 nm resulted from the reduced conjugated structure originated from the polymerization process. Notably, a blue-shifted wide shoulder peak at around 290 nm was observed, which could be assigned to the R–S_n–R groups.[15] SIVHP-1 and SIVHP-2 possess different feed molar ratios of S_8 to DIB of 8 and 2, respectively. UV-vis spectra of them showed different intensities because of their different amounts of R–S_n–R groups.

We further investigated the thermal properties of the SIVHPs. Curves of differential scanning calorimetry (DSC) are shown in Fig. 2b with different feed molar ratios (γ) of S_8 to DIB with 8, 4, 8/3 and 2. The corresponding glass transition temperatures (T_g) were 24.1 °C, 16.3 °C, 4.4 °C, and −0.5 °C, respectively. The T_g data of SIVHPs revealed that higher content of the utilized DIB led to lower T_g. When a higher feed molar ratio (γ) of S_8 to DIB was used, both of the C=C bonds in DIB would probably participate in the polymerization, introducing more rigid benzene rings into the molecular chain, thus higher T_g was obtained. On the contrary, smaller feed molar ratio led to less benzene rings in the molecular chains and lower T_g. TGA curves showed that SIVHPs and neat sulfur started to decompose at 170 °C (Fig. S4†), which made them difficult to be melting processed.

In general, we observed that SIVHPs were intrinsically orange-red (Fig. 3b), which originated from yellow-coloured sulfur (Fig. 3a). SIVHPs were dissolved in $CHCl_3$ (Fig. 3c) with the utmost concentration of 400 mg mL^{-1} at room temperature, and did not undergo any precipitation after settling for one month, superior to the limited solubility of bulk copolymers.

As shown in Fig. 3h and 3i, 15 mg of SIVHP could be dissolved in 2 mL of $CHCl_3$ within 5 minutes, while bulk

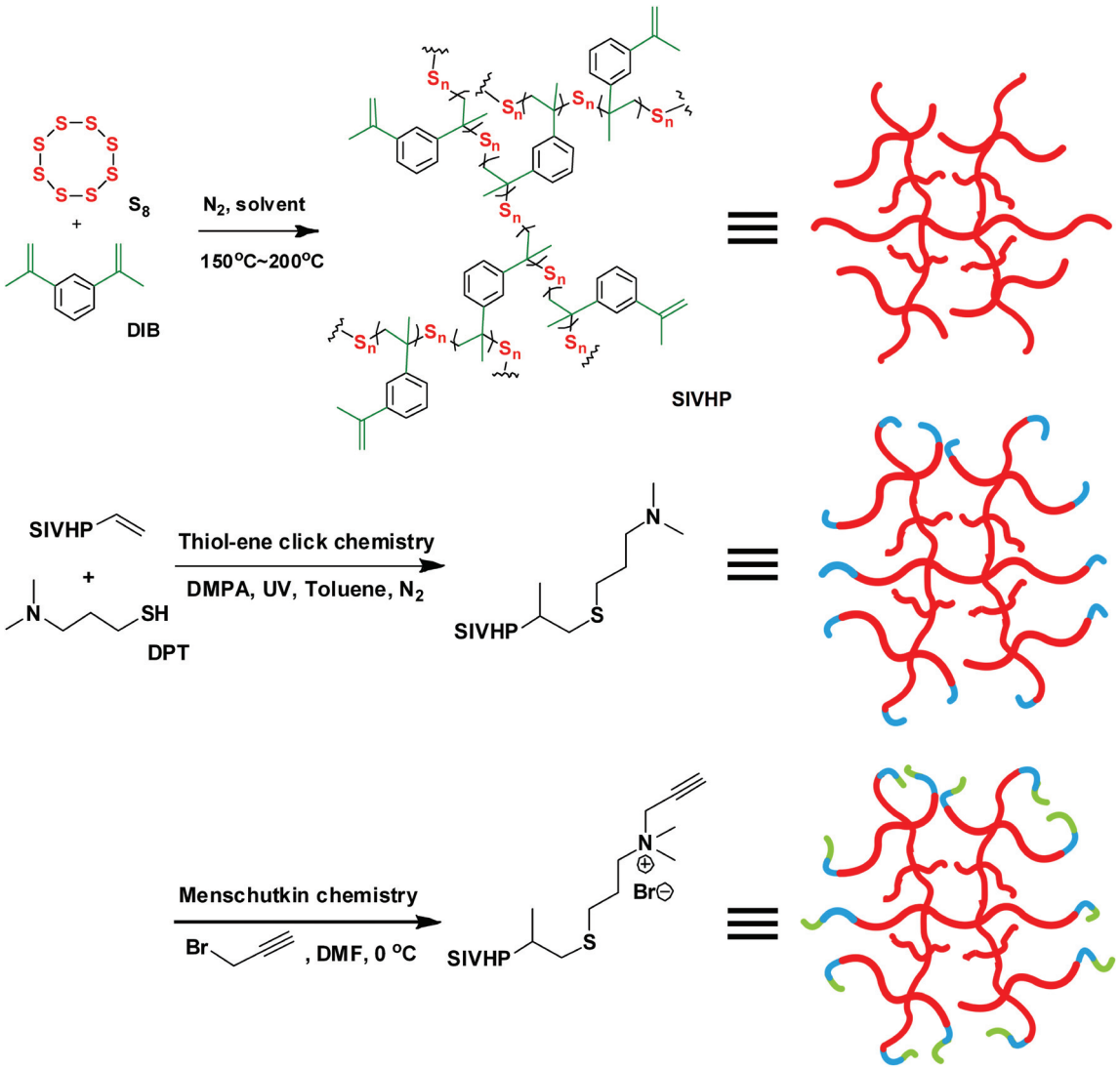

Scheme 1 Synthesis of SIVHPs *via* thiol–ene addition of polymeric S_8 radicals to DIB and subsequent functionalization by thiol–ene and Menschutkin click chemistry.

Table 1 Reaction conditions and selected results for the synthesis of SIVHPs *via* thiol–ene addition of polymeric S_8 radicals to DIB in $CHCl_3$

Entry	γ^a	Temperature/°C	Time/h	$M_n{}^b$ (g mol^{-1})	$M_w{}^b$ (g mol^{-1})	$M_p{}^b$ (g mol^{-1})	PDI^b
1	4 : 1	150	0.5	1300	2100	1200	1.62
2	4 : 1	160	0.5	1400	2400	1200	1.71
3	4 : 1	170	0.5	1500	2400	1400	1.60
4	4 : 1	180	0.5	5400	23 500	6200	4.35
5	4 : 1	190	0.5	2900	5100	2800	1.76
6	4 : 1	200	0.5	2600	6300	3000	2.42
7	4 : 1	180	0.25	1600	6500	1900	4.06
8	4 : 1	180	0.75	4200	18 200	5000	4.33
9	4 : 1	180	1	2800	7000	2800	2.50
10	4 : 1	180	2	2200	6200	2700	2.82
11	4 : 1	180	3	1900	3900	2400	2.05
12	4 : 1	180	5	1300	2500	1800	1.92
13	4 : 1	180	7	1100	2200	1600	2.00
14	8 : 1	180	0.5	2600	5300	2400	2.04
15	8 : 3	180	0.5	3000	5800	3100	1.93
16	8 : 4	180	0.5	2900	4300	3000	1.48
17	8 : 5	180	0.5	2700	3600	2900	1.33

[a] Feed molar ratios (γ) of S_8 to DIB. [b] Number-averaged molecular weight (M_n), weight-averaged molecular weight (M_w), peak value of M_n (M_p) and polydispersity index (PDI) determined by GPC.

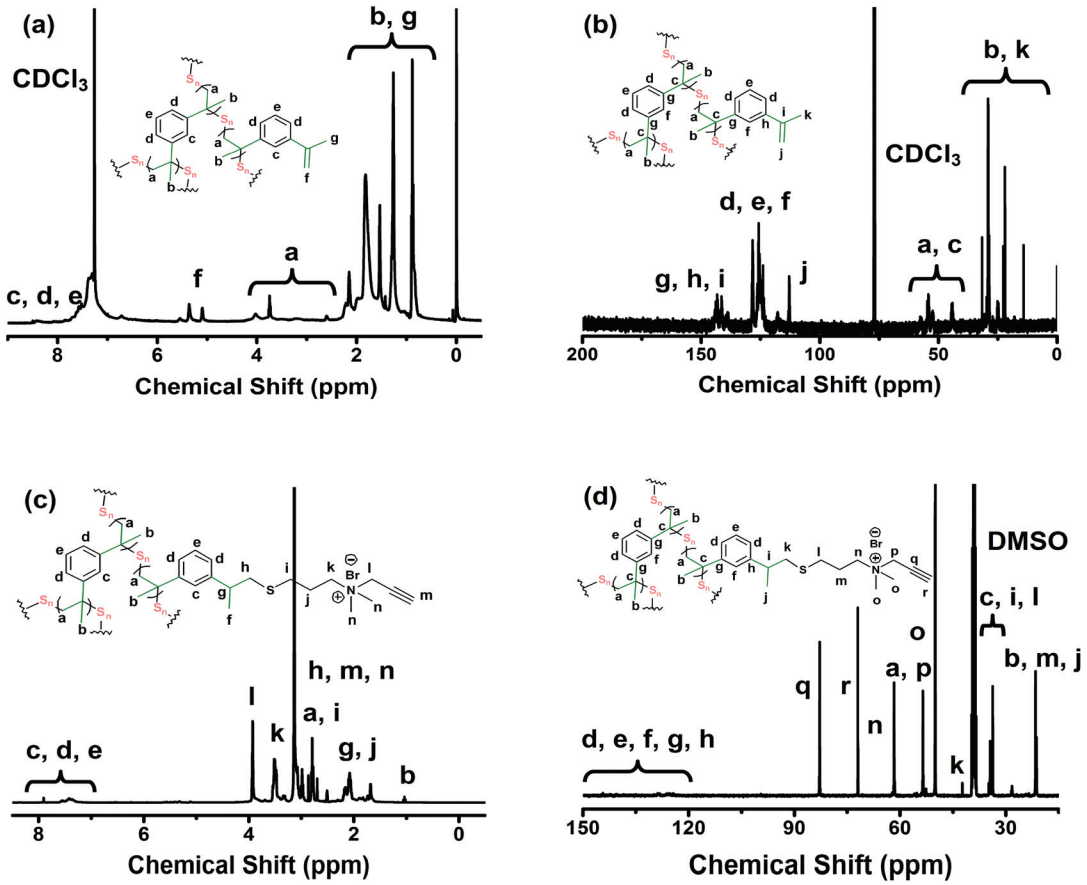

Fig. 1 (a) ^{1}H NMR spectrum of SIVHP in $CDCl_3$. (b) ^{13}C NMR spectrum of SIVHP in $CDCl_3$. (c) ^{1}H NMR spectrum of quaternary ammonium SIVHP in DMSO. (d) ^{13}C NMR spectrum of quaternary ammonium SIVHP in DMSO.

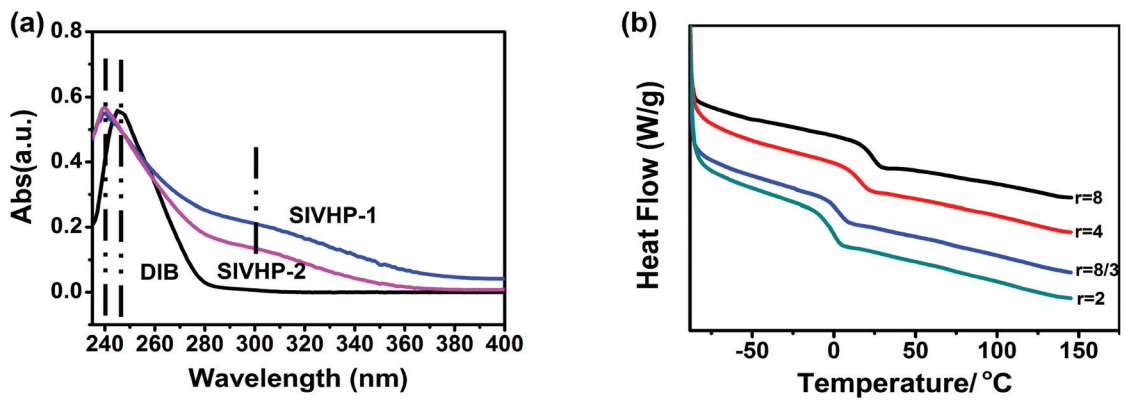

Fig. 2 (a) UV-Vis spectra of DIB and SIVHP-1 (feed molar ratio of S_8 to DIB was 8) and SIVHP-2 (feed molar ratio of S_8 to DIB was 2). (b) DSC of SIVHPs with feed molar ratios (γ = 8/5, 2, 8/3, 4, 8) of S_8 to DIB from 2 to 8, indicating the T_g of 24.1 °C, 16.3 °C, 4.4 °C, −0.5 °C, respectively.

copolymers of S_8 and DIB presented weaker and slower solubility with the same sulfur content of 70 wt% in polymers. The described SIVHPs presented good solubility in various organic solvents, such as toluene, $CHCl_3$, DMF, 1,4-dioxane, THF and anisole (Fig. 3j). In Fig. 3e, SIVHPs were spin-coated on the transparent substrate to form transparent films, which further elucidated their fine solution processability.

Synthesis and characterization of quaternary ammonium SIVHPs

SIVHPs presented excellent solubility in organic solvents but not in water. In this work, we synthesized functionalized quaternary ammonium SIVHPs with water-solubility for the first time *via* thiol–ene and Menschutkin reactions. The further

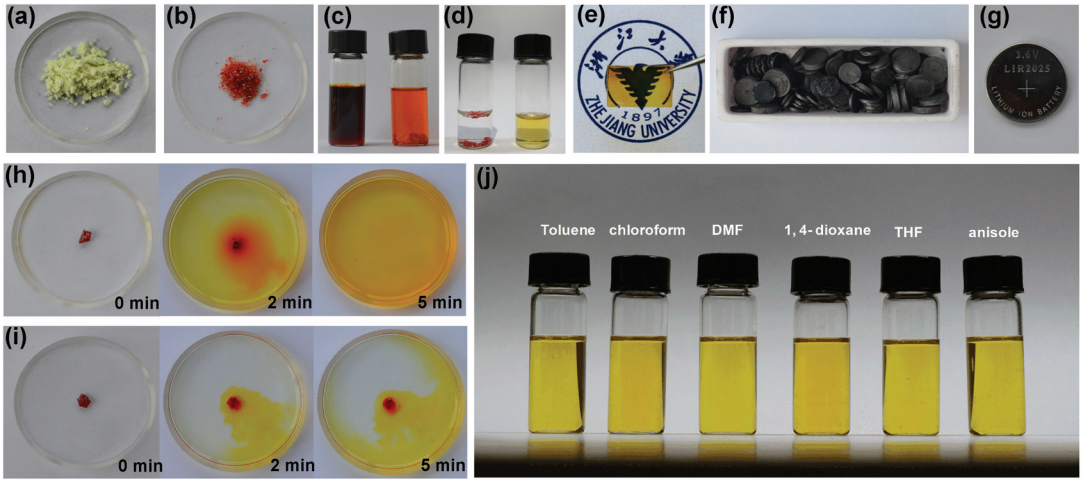

Fig. 3 Digital photographs of (a) sulfur, (b) SIVHP, (c) 800 mg SIVHP (left) and bulk polymer of S_8 and DIB (right) with 70 wt% sulfur content immersed in 2 mL chloroform at room temperature, (d) SIVHP (left) and quaternary ammonium SIVHP (right) immersed in water at room temperature, (e) film spin-coated with SIVHP solution on PET, (f) diverse-sized GUAs, (g) a Li–S battery we fabricated. Dissolution process of (h) SIVHP and (i) bulk polymer with the same feed molar ratios (γ) of S_8 to DIB within 5 min. (j) SIVHP dissolved in toluene, chloroform, DMF, 1,4-dioxane, THF and anisole.

chemical functionalization to tune the composition and properties was based on the high solubility and hyperbranched structure. SIVHPs were modified with sulfhydryl through thiol–ene click chemistry of thiols and C=C bonds under UV initiation, followed by Menschutkin click reaction with propargyl bromide. The reaction mechanism is shown in Scheme 1.[16]

Different from SIVHPs, the quaternary ammonium SIVHPs showed superior solubility in water, which directly demonstrated the chemical conversion from SIVHPs to quaternary ammonium SIVHPs (Fig. 3d). The structures of quaternary ammonium SIVHPs were characterized *via* ^{1}H NMR and ^{13}C NMR spectroscopy shown in Fig. 1c and 1d. In the ^{1}H NMR spectrum (Fig. 1c), the disappearance of vinyl protons and the proton signal of alkynyl protons proved that functionalization was successfully completed. In the ^{13}C NMR spectrum (Fig. 1d), the alkynyl carbon signal labelled as "r" located at 71.97 ppm also implied the successful modification. The molar masses before and after modification almost kept consistent (Table S1†), indicating that the framework of SIVHPs is stable during the chemical reaction. In short, SIVHPs had the capacity to be modified, and offered a larger range of solution processability and new opportunities to fabricate water-soluble, amphiphilic sulfur-rich species.

Electrochemical measurements

Li–S batteries are receiving interest for their outstanding merits such as the ultrahigh theoretical energy capacity of 1672 mA h g^{-1}, the high theoretical specific energy of 2600 W h kg^{-1} and environmentally friendly operation.[17] However, intermediate lithium polysulfides, which are generated from stepwise reduction reactions during the discharge processes, would dissolve in the liquid electrolytes and shuttle between the anode and cathode.[18] The shuttle effect, along with the raised resistance of sulfur, intensively degraded the stability and increased the pointless cost of sulfur-active materials.[19] Due to all these problems, a big gap existed between practical performance and theoretical expectation upon cycle life, specific capacity and energy efficiency of Li–S batteries.[20]In view of the excellent solution processability of the SIVHPs, they were assembled into conductive frameworks of GUAs by facile fluid infiltration, playing the role of cathode-active materials in Li–S batteries. The GUAs previously reported by our group were constructed with cell walls of giant graphene sheets and CNTs ribs, which possessed superior electroconductivity, large surface area (~272 m^2 g^{-1}), and super-high absorption capacities for organic solvents.[7] In order to achieve strong skeletons and dense holes, we fabricated GUAs with a density of 6.0 mg mL^{-1} (Fig. 3f). Element mapping images and energy-dispersive X-ray (EDX) analysis further illuminated the homogeneous and abundant distribution of sulfur in GUAs (Fig. 4), indicating effective infiltration of SIVHPs along the walls of the aerogels. An efficient connected network would improve the electrical conductivity of the cathode materials, and thus improve the charge–discharge efficiency.[21]

Coin cells (2025, Fig. 3g) consisting of Li-foil anodes and SIVHPs-GUAs composite cathodes were tested to examine the electrochemical performance. The content of sulfur in SIVHPs was determined to be ~75 wt% by TGA (Fig. 4f).

An initial specific discharge capacity of 1247.6 mA h g^{-1} with long-term cycle stability of 400 cycles is shown in Fig. 5c at a rate of 0.1 C (1 C = 1672 mA g^{-1}), which outdistanced the performance of pure sulfur. The solubility of SIVHPs in electrolyte was examined, and the results are listed in Table S2.† SIVHPs showed low solubility in electrolyte. The poor solubility of SIVHPs in electrolyte implied their stability in the liquid

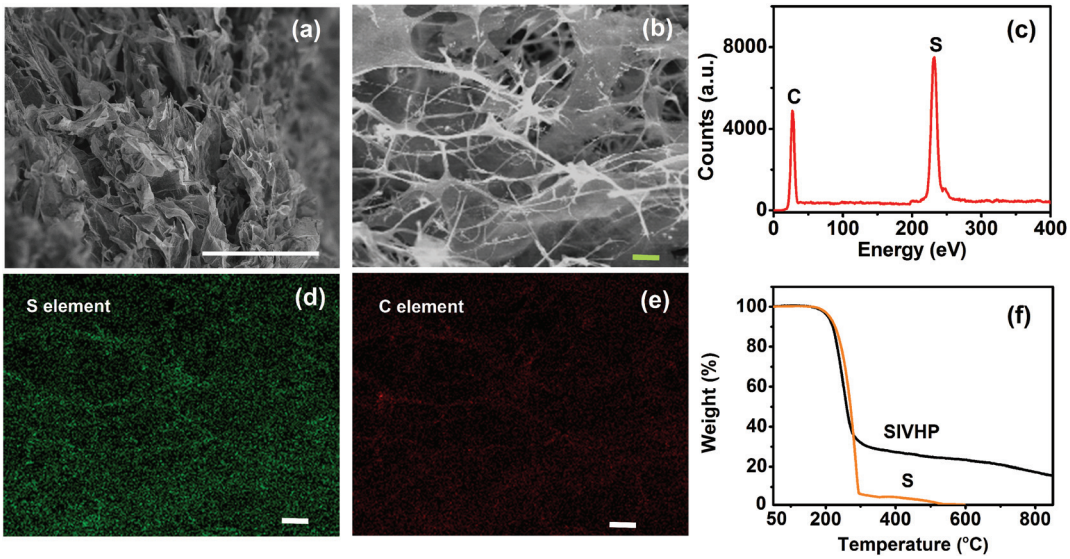

Fig. 4 (a) SEM image of GUAs (ρ = 6 mg mL^{-3}), (b) SEM image of SIVHPs-GUAs composite. (c) EDX spectrum of SIVHPs-GUAs composite. (d) Elemental mapping of sulfur. (e) Elemental mapping of carbon. (f) TGA curves measured for sulfur and SIVHP. Scale bars are 50 μm (a) and 10 μm (b, d, e).

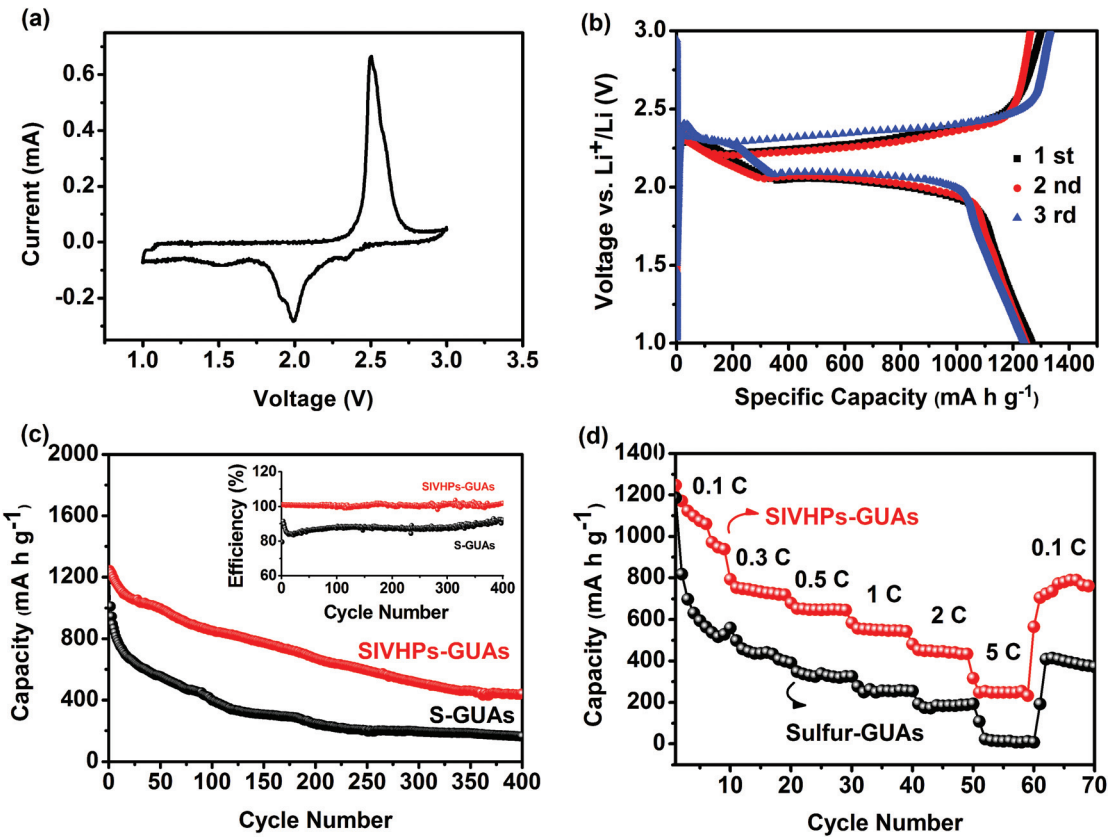

Fig. 5 Electrochemical measurements of SIVHPs-GUAs as Li–S battery cathode materials. (a) Cyclic voltammetry of SIVHPs-GUAs at 0.1 mV s^{-1} in a potential window from 1.0 to 3.0 V *vs.* Li$^+$/Li. (b) Charge/discharge profiles of the SIVHPs-GUAs cathode at a current rate of 0.1 C. (c) Galvanic charge–discharge performance of sulfur and SIVHPs-GUAs at 0.1 C for 400 cycles, and inset for coulombic efficiency of SIVHPs-GUAs at 0.1 C for 400 cycles. (d) Rate capabilities of SIVHPs-GUAs and S-GUAs composite cathodes.

electrolyte used. The loss of capacity during the initial 10 cycles may be attributed to the permeation through the separators and deposition on anode of intermediates which dissolved in the electrolyte during discharge. The process resulted in irreversible loss of the active material and capacity.

In order to explore the mechanism, CV of the cells were tested with a scan rate of 0.1 mV s^{-1} between 1.0 and 3.0 V *versus* Li/Li^+, which were made with SIVHPs-GUAs as the cathode-active materials (Fig. 5a). The reduction peaks at potentials of 2.3 V and 2.0 V respectively corresponded to the formation of long-chain Li_2S_n ($4 \leq n \leq 8$) and lower-order Li_2S_n ($2 \leq n \leq 4$). The broad reduction current peak at ~1.5 V suggested a solid-to-solid phase transition (from SIVHP to Li_2S). In the anodic scan, only one oxidation peak at 2.5 V was observed, which was related to the conversion of Li_2S and/or short-chain polysulfides to long-chain polysulfides.[22] Fig. 5b showed the galvanostatic charge/discharge curves in the 1st, 2nd and 3rd cycles at a current rate of 0.1 C. Corresponding to the CV profiles, two plateaus were assigned to the formation of long-chain polysulfides (high plateau at 2.3 V) and lower-order Li_2S_n (low plateau at 2.0 V) during the discharge process.

Notably, the coulombic efficiencies of SIVHPs-GUAs at 0.1 C were all around 100% during 400 cycles (Fig. 5c, inset). In contrast, sulfur-GUAs exhibited low coulombic efficiency from 91.5 to 83.5%, which was caused by a serious shuttle effect due to the lack of chemical fixation of neat sulfur.[23] Galvanic current measurements were taken to evaluate the rate performance of the SIVHPs-GUAs and sulfur-GUAs composite electrodes (Fig. 5d). SIVHPs-GUAs showed capacities of 1217, 796, 685, 583, 482, and 255 mA h g^{-1} at the current rates of 0.1, 0.3, 0.5, 1, 2 and 5 C after 10 cycles, respectively. In addition, after the rate test for 60 cycles, a discharge capacity of 800 mA h g^{-1} was maintained when it returned to 0.1 C. By contrast, neat sulfur-GUAs exhibited a rapid and massive loss of capacities (1192, 506, 348, 284, 196 and 27 mA h g^{-1} at current rates of 0.1, 0.3, 0.5, 1, 2 and 5 C, respectively, after 10 cycles). We proposed that the good performance of the SIVHPs-GUAs composite electrode was attributed to the chemical fixation of sulfur *via* hyperbranched polymerization. It should be mentioned that the function of GUAs is to construct a three-dimensional network substantially and improve the electroconductibility of the cathode material, which was supported by the electrochemical impedance spectra (EIS) measurements (Fig. S5†). The smaller diameter of the semicircle, which corresponds to smaller charge-transfer resistance, showed better electroconductibility of the SIVHPs-UFAs electrode and verified our comprehension.[24] All these results demonstrated the advantage to design SIVHPs with high processability and combine sulfur-rich polymers with porous conductive carbon.

Conclusions

In this work, we prepared soluble inverse-vulcanized hyperbranched polymers *via* facile thiol–ene addition of S_8 radicals to DIB in solution. Modification *via* thiol–ene and Menschutkin reactions endowed the sulfur-rich polymers with water solubility for the first time, which was based on the high solubility and the structure of hyperbranched molecule. The hyperbranched polymers were proved to be solution processible and possessed good electrochemical performance exceeding neat sulfur. In view of the attributes of large surface area and electroconductibility, we introduced graphene-CNTs aerogels to support the hyperbranched polymers as new cathode-active materials in Li–S batteries. The synthetic method and sulfur-rich polymers with hydrophilic and oleophilic properties would bring new ideas for the design of Li–S batteries. Due to their high solubility, excellent solution processability, clickable multifunctional groups, and superior electrochemical performance, the sulfur-rich hyperbranched polymers are promising in many applications such as Li–S batteries, host–guest encapsulation, and drugs.

Acknowledgements

This work is supported by the National Natural Science Foundation of China (no. 51173162 and no. 21325417), Fundamental Research Funds for the Central Universities (no. 2013XZZX003), and China Postdoctoral Science Foundation (2014M551724).

Notes and references

1 P. Flory, *J. Am. Chem. Soc.*, 1952, **74**, 2718; C. Gao and D. Y. Yan, *Prog. Polym. Sci.*, 2004, **29**, 183; D. Yan, C. Gao and H. Frey, *Hyperbranched Polymers: Synthesis, Properties and Applications*, John Wiley & Sons, Hoboken, NJ, 2011; B. Voit, *J. Polym. Sci., Part A: Polym. Chem.*, 2000, **38**, 2505; M. Jikei and M. Kakimoto, *Prog. Polym. Sci.*, 2001, **26**, 1233; C. Gao, S. Muthukrishnan, W. Li, J. Yuan, Y. Xu and A. H. E. Müller, *Macromolecules*, 2007, **40**, 1803.

2 C. C. Lee, J. A. MacKay, J. M. J. Fréchet and F. C. Szoka, *Nat. Biotechnol.*, 2005, **23**, 1517; Y. K. Jeong, T. W. Kwon, I. Lee, T. S. Kim, A. Coskun and J. W. Choi, *Nano Lett.*, 2014, **14**, 864; Y. Liang, Z. Tao and J. Chen, *Adv. Energy Mater.*, 2012, **2**, 742; D. M. Tigelaar, M. A. B. Meador, J. D. Kinder and W. R. Bennett, *Macromolecules*, 2006, **39**, 120; T. Itoh, Y. Ichikawa, T. Uno, M. Kubo and O. Yamamoto, *Solid State Ionics*, 2003, **156**, 393.

3 J. M. Tarascon and M. Armand, *Nature*, 2001, **414**, 359; A. S. Aricò, P. Bruce, B. Scrosati, J. M. Tarascon and W. V. Schalkwijc, *Nat. Mater.*, 2005, **4**, 366; P. G. Bruce, B. Scrosati and J. M. Tarascon, *Angew. Chem., Int. Ed.*, 2008, **47**, 2930; M. S. Whittingham, *Chem. Rev.*, 2004, **104**, 4271; S. S. Zhang, *Front. Energy Res.*, 2013, **1**, 10.

4 K. Naoi, K. I. Kawase, M. Mori and M. Komiyama, *J. Electrochem. Soc.*, 1997, **144**, L173; F. Wu, S. X. Wu, R. J. Chen, J. Z. Chen and S. Chen, *Electrochem. Solid-State Lett.*, 2010, **13**, A29; S. Zhang, *Energy Storage*, 2013, **1**, 10.

5 J. Wang, J. Yang, C. Wan, K. De, J. Xie and N. Xu, *Adv. Funct. Mater.*, 2003, **13**, 487; L. Xiao, Y. Cao, J. Xiao, B. Schwenzer, M. H. Engelhard, L. V. Saraf, Z. Nie, G. J. Exarhos and J. Liu, *Adv. Mater.*, 2012, **24**, 1176; Y. NuLi, Z. Guo, H. Liu and J. Yang, *Electrochem. Commun.*, 2007, **9**, 1913.

6 W. J. Chung, J. J. Griebel, E. T. Kim, H. Yoon, A. G. Simmonds, H. J. Ji, P. T. Dirlamk, R. S. Glass, J. J. Wie, N. A. Nguyen, B. W. Guralnick, J. Park, á. Somogyi, P. Theato, M. E. Mackay, Y. E. Sung, K. Char and J. Pyun, *Nat. Chem.*, 2013, **5**, 518; J. J. Griebel, S. Namnabat, E. T. Kim, R. Himmelhuber, D. H. Moronta, W. J. Chung, A. G. Simmonds, K. Kim, J. Laan, N. A. Nguyen, E. L. Dereniak, M. E. Mackay, K. Char, R. S. Glass, R. A. Norwoodand and J. Pyun, *Adv. Mater.*, 2014, **26**, 3014; A. G. Simmonds, J. J. Griebel, J. Park, K. R. Kim, W. J. Chung, V. P. Oleshko, J. Kim, E. T. Kim, R. S. Glass, C. L. Soles, Y. Sung, K. Char and J. Pyun, *ACS Macro Lett.*, 2014, **3**, 229; J. J. Griebel, G. Li, R. S. Glass, K. Char and J. Pyun, *J. Polym. Sci., Part A: Polym. Chem.*, DOI: 10.1002/pola.27314.

7 H. Sun, Z. Xu and C. Gao, *Adv. Mater.*, 2013, **25**, 2554; Z. Xu and C. Gao, *Acc. Chem. Res.*, 2014, **47**, 1267.

8 Z. Sun, M. Xiao, S. Wang, D. Han, S. Song, G. Chen and Y. Meng, *J. Mater. Chem. A*, 2014, **2**, 9280.

9 Z. Xu, H. Sun and C. Gao, *Appl. Mater.*, 2013, **1**, 030901; T. Huang, B. Zheng, L. Kou, K. Gopalsamy, Z. Xu, C. Gao, Y. Meng and Z. Wei, *RSC Adv.*, 2013, **3**, 23957; Z. Xu, H. Sun, X. Zhao and C. Gao, *Adv. Mater.*, 2013, **25**, 188; Z. Xu, Y. Zhang, P. Li and C. Gao, *ACS Nano*, 2012, **6**, 7103; Z. Xu and C. Gao, *ACS Nano*, 2011, **5**, 2908; L. Kou, T. Huang, B. Zheng, Y. Han, X. Zhao, K. Gopalsamy and C. Gao, *Nat. Commun.*, 2014, **5**, 3754.

10 C. Gao, S. Muthukrishnan, W. Li, J. Yuan, Y. Xu and A. H. E. Müller, *Macromolecules*, 2007, **40**, 1803; C. Gao, D. Yan and W. Chen, *Macromol. Rapid Commun.*, 2002, **23**, 465; Y. Han, C. Gao and X. He, *Sci. China: Chem.*, 2012, **55**, 604; S. Li and C. Gao, *Polym. Chem.*, 2013, **4**, 4450; J. Han, S. Li and C. Gao, *Macromolecules*, 2012, **45**, 4966.

11 E. J. Goethals, *J. Macromol. Sci., Part C*, 1968, **2**, 1; H. W. Nesbitt, G. M. Bancroft, A. R. Pratt and M. J. Scaini, *Am. Mineral*, 1998, **83**, 1067; R. Bellissent, L. Descotes and P. Pfeuty, *J. Phys.: Condens. Matter*, 1994, **6**, A211; J. S. Tse and D. D. Klug, *Phys. Rev. B: Condens. Matter*, 1999, **59**, 34; R. Steudel, *Chem. Rev.*, 2002, **102**, 3905; L. B. Blight, B. R. Currell, B. J. Nash, R. T. M. Scott and C. Stillo, *Br. Polym. J.*, 1980, **12**, 5.

12 A. M. Fischer and H. Frey, *Macromolecules*, 2010, **43**, 8539; N. Clarke, E. D. Luca, J. M. Dodds, S. M. Kimani and L. R. Hutchings, *Eur. Polym. J.*, 2008, **44**, 665; X. Zhou, J. Zhu, M. Xing, Z. Zhang, Z. Cheng, N. Zhou and X. Zhu, *Eur. Polym. J.*, 2011, **47**, 1912.

13 E. J. Goethals, *Topics in Sulfur Chemistry*, Georg Thieme Verlag, Stuttgart, 1977; S. P. Li, J. Han and C. Gao, *Polym. Chem.*, 2013, **4**, 1774; H. Sun and C. Gao, *Biomacromolecules*, 2010, **11**, 3609; J. Han, B. Zhao, Y. Gao, A. Tang and C. Gao, *Polym. Chem.*, 2011, **2**, 2175.

14 E. Prestch, P. Bühlmann and C. Affolter, *Structure Determination of Organic Compounds: Table of Spectra Data*, Springer-Verlag, Berlin Heidelberg, New York, 3rd edn, 2000; I. Garcia-Lodeiro, A. Fernandez-Jimenez, M. T. Blanco-Varela and A. Palomo, *J. Sol-Gel Sci. Technol.*, 2008, **45**, 63.

15 C. Barchasz, F. Molton, C. Duboc, J. C. Leprêtre and S. Patoux, *Anal. Chem.*, 2012, **84**, 3973; Y. Li, H. Zhan, S. Liu, K. Huang and Y. Zhou, *J. Power Sources*, 2010, **195**, 2945; M. U. M. Patel, R. Demir-Cakan, M. Morcrette, J. M. Tarascon, M. Gaberscek and R. Dominko, *ChemSusChem*, 2013, **6**, 1177; L. Wang, X. He, J. Li, J. Gao, J. Guo, C. Jiang and C. Wan, *J. Mater. Chem.*, 2012, **22**, 22077; J. Rong, M. Ge, X. Fang and C. Zhou, *Nano Lett.*, 2014, **14**, 473.

16 J. Han, Y. Zheng, S. Zheng, S. Li, T. Hu, A. Tang and C. Gao, *Chem. Commun.*, 2014, **50**, 8712.

17 A. Manthiram, Y. Fu and Y. S. Su, *Acc. Chem. Res.*, 2012, **46**, 1125; S. Xin, Y. G. Guo and L. J. Wan, *Acc. Chem. Res.*, 2012, **45**, 1759; B. Scrosati and J. Garche, *J. Power Sources*, 2010, **195**, 2419; P. G. Bruce, S. A. Freunberger, L. J. Hardwick and J. M. Tarascon, *Nat. Mater.*, 2012, **11**, 19; S. S. Zhang and J. A. Read, *J. Power Sources*, 2012, **200**, 77; C. Liang, N. J. Dudney and J. Y. Howe, *Chem. Mater.*, 2009, **21**, 4724.

18 R. Chen, T. Zhao, J. Lu, F. Wu, L. Li, J. Chen, G. Tan, Y. Ye and K. Amine, *Nano Lett.*, 2013, **13**, 4642; N. S. Choi, Z. Chen, S. A. Freunberger, X. Ji, Y. K. Sun, K. Amine, G. Yushin, L. F. Nazar, J. Cho and P. G. Bruce, *Angew. Chem., Int. Ed.*, 2012, **51**, 9994; Y. X. Yin, S. Xin, Y. G. Guo and L. Wan, *Angew. Chem., Int. Ed.*, 2013, **52**, 13186.

19 S. Evers and L. F. Nazar, *Acc. Chem. Res.*, 2012, **46**, 1135; G. Zhou, S. Pei, L. Li, D. Wang, S. Wang, K. Huang, L. Yin, F. Li and H. Cheng, *Adv. Mater.*, 2014, **26**, 625; L. Ji, M. Rao, H. Zheng, L. Zhang, Y. Li, W. Duan, J. Guo, E. J. Cairnsand and Y. Zhang, *J. Am. Chem. Soc.*, 2011, **133**, 18522; S. S. Zhang, *J. Power Sources*, 2013, **231**, 153; S. Evers and L. F. Nazar, *Acc. Chem. Res.*, 2013, **46**, 1135.

20 H. Wang, Y. Yang, Y. Liang, J. T. Robinson, Y. Li, A. Jackson, Y. Cui and H. Dai, *Nano Lett.*, 2011, **11**, 2644; A. G. Simmonds, J. J. Griebel, J. Park, K. R. Kim, W. J. Chung, V. P. Oleshko, J. Kim, E. T. Kim, R. S. Glass, C. L. Soles, Y. E. Sung, K. Char and J. Pyun, *ACS Macro Lett.*, 2014, **3**, 229.

21 Y. Yang, G. Zheng and Y. Cui, *Chem. Soc. Rev.*, 2013, **42**, 3018; Y. Yang, G. Zheng and Y. Cui, *Chem. Soc. Rev.*, 2013, **42**, 3018; X. Ji, K. T. Lee and L. F. Nazar, *Nat. Mater.*, 2009, **8**, 500; N. Li, M. Zheng, H. Lu, Z. Hu, C. Shen, X. Chang, G. Ji, J. Cao and Y. Shi, *Chem. Commun.*, 2012, **48**, 4106; B. Zhang, X. Qin, G. Li and X. Gao, *Energy Environ. Sci.*, 2010, **3**, 153.

22 F. Wu, J. Chen, R. Chen, S. Wu, L. Li, S. Chen and T. Zhao, *J. Phys. Chem. C*, 2011, **115**, 6057; J. Liu, T. Yang, D. Wang, G. Lu, D. Zhao and S. Qiao, *Nat. Commun.*, 2013, **4**, 2798; W. Zhou, H. Chen, Y. Yu, D. Wang, Z. Cui, F. J. DiSalvo and H. D. Abruña, *ACS Nano*, 2013, **7**, 8801; M. Q. Zhao,

X. F. Liu, Q. Zhang, G. L. Tian, J. Q. Huang, W. Zhu and F. Wei, *ACS Nano*, 2012, **6**, 10759.

23 L. Suo, Y. Hu, H. Li, M. Armand and L. Chen, *Nat. Commun.*, 2013, **4**, 1481; Y. Cao, X. Li, I. A. Aksay, J. Lemmon, Z. M. Nie, Z. G. Yang and J. Liu, *Phys. Chem. Chem. Phys.*, 2011, **13**, 7660; X. Liang, Z. Wen, Y. Liu, H. Zhang, L. Huang and J. Jin, *J. Power Sources*, 2011, **196**, 3655.

24 D. Aurbach, I. Weissman, A. Zaban, Y. Ein-Eli, E. Mengeritsky and P. Dan, *J. Electrochem. Soc.*, 1996, **143**, 2110; L. Yuan, H. Yuan, X. Qiu, L. Chen and W. Zhu, *J. Power Sources*, 2009, **189**, 1141.